BMC Veterinary Research

RESEARCH

Open Access

Lumpy skin disease virus ORF142 protein inhibits type I interferon production by disrupting interactions of TBK1 and IRF3

Zihan Chen[1], Jingyu Wang[1], Baochun Lu[2], Heyu Li[1], Chuanli Liu[1], Huijuan Zeng[1], Jinping Chen[1], Shizhe Liu[1], Qifeng Jiang[1] and Kun Jia[1*]

Abstract

Background Lumpy skin disease virus (LSDV) causes lumpy skin disease, which is one of the most devastating ruminant diseases. The pathogenesis of the disease remains largely unknown; however, the disease seriously threatens the global cattle-farming industry. In our previous study, we found that LSDV 142 gene deletion affected LSDV proliferation in cells and was an early gene involved in LSDV infection. Additionally, the study found that ORF142 inhibits the production of interferon beta.

Results Herein, we report that LSDV inhibits the host antiviral response. The results revealed that the LSDV ORF142 protein inhibited interferon-promoter activation. ORF142 suppresses the host antiviral response by blocking interferon beta (IFN-β) production based on 381–417 amino acids at the C-terminal domain site of interferon regulatory factor 3 (IRF3). ORF142 interacts with IRF3 and interferes with the recruitment of IRF3 to TANK-binding kinase 1 (TBK1) in a dose-dependent manner, preventing nuclear translocation of IRF3.

Conclusions These results suggest that LSDV ORF142 antagonizes host antiviral innate immunity by affecting the binding between TANK-binding kinase 1 and IRF3. Our findings provide new information regarding the pathogenesis of this virus.

Keywords LSDV, ORF142, IRF3, TBK1, Immune evasion

Background

Lumpy skin disease (LSD) is an acute or subacute contact infection caused by the lumpy skin disease virus (LSDV), which is characterized by fever and extensive nodules or ulceration of the skin and internal organs in cattle. Recently, LSD has become one of the most devastating diseases affecting large domesticated ruminants, such as cattle, buffalo, and bison. The World Organization for Animal Health has classified LSD as one of the most economically important animal diseases, making it a notifiable transboundary animal virus [1].

LSDV is a double-stranded DNA virus, which is a member of the *Capripoxvirus* genus of *Poxviridae*, *Sheeppox virus* [2], approximately 270 nm × 290 nm in size, with only one serotype and no coagulant activity [3]. The total length of the LSDV genome is 145–156 kbp and consists of up to 156 open reading frames (ORFs) [4]. LSDV contains the most conserved poxvirus genes related to viral replication, including at least 26 genes

*Correspondence:
Kun Jia
jiakun@scau.edu.cn
[1]College of Veterinary Medicine, South China Agricultural University, Guangdong 510642, China
[2]College of Veterinary Medicine, Jilin University, Changchun 130062, China

involved in RNA polymerase subunits, mRNA transcription initiation, extension, and termination, and enzymes that must be modified or processed after viral mRNA transcription [5].

Viral infections are sensed by pattern recognition receptors (PRRs) that recognize viral particle components or replicate viral infection by-products and upregulate interferon-stimulated genes (ISGs) by promoting the production of type I interferons (IFNs) [6]. IFN-I production is a key component of the body's innate immunity to viruses, and the most widely studied IFN-I in virus-infected cells are interferon alpha (IFN-α) and interferon beta (IFN-β) [7]. ISGs are categorized into proinflammatory and antiviral. Proinflammatory ISGs recruit immune effector cells, whereas antiviral ISGs produce antiviral factors in and around virus-infected cells, thus limiting viral transmission [8]. LSDV belongs to an evolutionarily conserved family of the *Sheeppox virus* with more than 90% homology to other members of the *Goatpox virus* and *Sheeppox virus* genera [9]. Retinoic Acid-inducible Gene-I (RIG-I) has been shown to be an important PRR in the innate immune activation signaling pathway during *Sheeppox virus* infection [10]. In 2024, Liang et al. elucidated that the LSDV *ORF127* gene suppressed IFN-β expression through the cGAS-STING signaling pathway [11]. These studies have laid the foundation for studying the mechanisms of LSDV evasion of innate immunity.

TANK-binding kinase 1 (TBK1) is a multifunctional protease that mediates the activation of interferon regulatory factor 3/7 (IRF3/7) [12, 13] and translocates to the nucleus [14] during the innate immune response, thus inducing IFN-I production, with IRF3 primarily promoting IFN-β production [15]. Human Immunodeficiency Virus (HIV) infection induces cGAS-STING-TBK1-IRF3 signaling to activate innate immunity and produce IFN-I by enhancing the interaction of the nonstructural protein viral infection factor with the cellular tyrosine phosphatase SHP-1 via the immunoreceptor tyrosine motif (ITIM) [16]. Waveform proteins interact with TBK1 and IKKε to disrupt the TBK1-IRF3 and IKKε-IRF3 interactions, thus inhibiting RNA and DNA virus-induced IFN-I production [17]. The African Swine Fever Virus (ASFV) structural protein E120R evades the host's antiviral immune response by inhibiting the TBK1-IRF3 pathway [18]. These results suggest that viral proteins act on the TBK1-IRF3 axis to evade host innate immunity.

The LSDV 142 gene consists of 133 amino acids [19]. Pre-experimental assays indicated that ORF142 encodes a protein that inhibits IFN-β. However, the precise molecular mechanisms by which ORF142 exerts its inhibitory effects on IFN-I production remain poorly understood. Furthermore, while it is known that LSDV 142 gene deletion impacts viral proliferation and that ORF142 is an early gene involved in LSDV infection, the specific interactions between ORF142 and host immune signaling pathways have not been fully elucidated. LSDV 142 gene deletion affects LSDV proliferation in cells, and LSDV 142 is an early gene involved in LSDV infection. In this study, we show that LSDV ORF142 restricts nuclear translocation by inhibiting the interaction of TBK1 with IRF3, thus attenuating the production of IFN-I. The potential mechanism by which LSDV inhibits IFN-I production is important for the development of live attenuated vaccines and for the prevention and control of LSD.

Results

ORF142 inhibits IRF3-5D-mediated IFN-β production

To confirm whether LSDV ORF142 regulates IFN-I production, we transfected Flag-IRF3, HA-IRF3-5D, and GFP-ORF142 into HEK-293T cells, and by RT-qPCR assay, we found that ORF142 significantly inhibited IRF3 active form (IRF3-5D)-induced IFN-β, ISG15, ISG54, and ISG56 expression (Fig. 1A–D). To confirm the effect of LSDV ORF142 on IFN-I activation, we assessed the effect of ORF142 on IFN-I and ISRE luciferase reporter plasmids using the DLR gene assay. HEK-293T cells were co-transfected with the IFN-β-Luc reporter gene, ISRE-Luc reporter gene, and pRL-TK expression plasmid, harvested, and analyzed for luciferase activity after 24 h. ORF142 significantly inhibited the activation of the IFN-I and ISRE promoters (Fig. 1E–F).

IRF3 interacts with ORF142 during viral infection

IRF3 is the main transcription factor that induces IFN-I [20]. These results show that LSDV ORF142 inhibits the IRF3 mediated IFN-β production. We hypothesized that there is a relationship between ORF142 and IRF3. We transfected GFP-ORF142 with mCherry-IRF3 and vec-mCherry (empty mCherry) into 293T cells and analyzed them with a co-immunoprecipitation assay (Co-IP) after 24 h. GFP-ORF142 was immunoprecipitated with mCherry-IRF3 (Fig. 2A), indicating that ORF142 interacts with IRF3.

In addition to probing the structural domains required for IRF3 to interact with ORF142, we generated three truncation mutants of IRF3: M1 (1-186 aa), which is 21 kDa; M2 (187–380 aa), which is 22 kDa; M3 (381–417 aa), which is 4 kDa; and M4 (1-417 aa), which is full-length (Fig. 2B). The truncate was ligated to the mCherry vector and co-transfected into 293T cells with GFP-ORF142. After 24 h, cell lysates were immunoprecipitated using magnetic beads containing anti-GFP antibody and analyzed by western blotting (Fig. 2C). The results revealed that, although ORF142 effectively downregulated IRF3-M3 (Fig. 2C orange arrow), it did not interact with IRF3-M1 (Fig. 2C blue arrow), and IRF3-M2 (Fig. 2C green arrow). Confocal microscopy revealed that ORF142 interacted with IRF3-M3 (Fig. 2D), which was

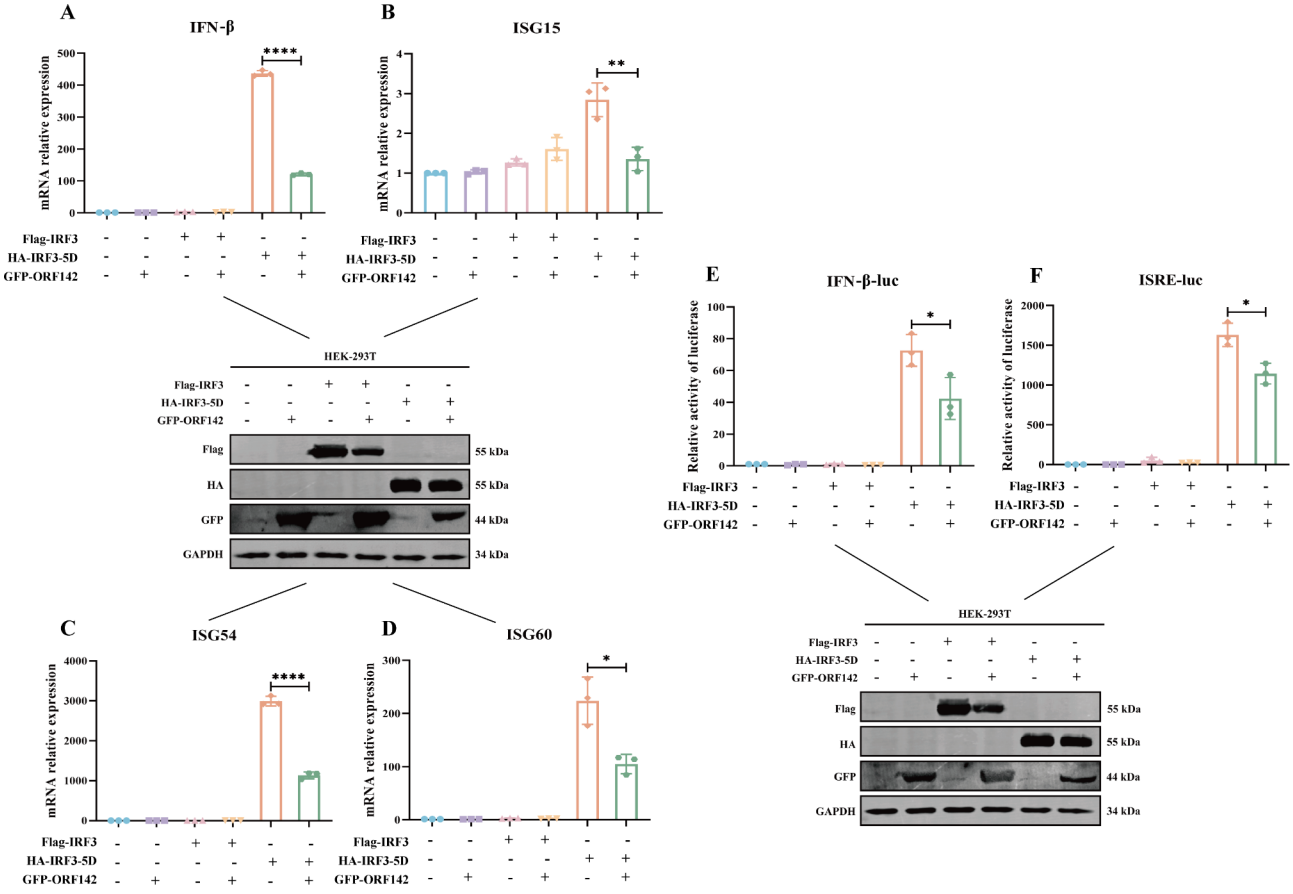

Fig. 1 LSDV ORF142 inhibits activated IRF3 (IRF3-5D)-induced IFN-I production. (**A**–**D**) GFP-ORF142 was co-transfected with Flag-IRF3 and HA-IRF3-5D (activated IRF3), and total cellular RNA was extracted after 24 h. The mRNA expression levels of IFN-β (**A**), ISG15 (**B**), ISG54 (**C**), and ISG60 (**D**) were determined by RT-qPCR. (**E** and **F**) GFP-ORF142 was co-transfected with Flag-IRF3, HA-IRF3-5D (activated IRF3), IFNβ-Luc, and ISRE-Luc into 293T cells, and luciferase activity was evaluated after 24 h. The data represent the mean ± standard deviation of three independent experiments. GraphPad was used to determine the statistical significance and create the graphs. *$P < 0.05$, **$P < 0.01$, ***and ****$P < 0.001$.

consistent with the Co-IP results. The aforementioned results suggest that ORF142 inhibits the nuclear translocation of IRF3 and interacts with the amino acid region 381-417aa in IRF3.

Inhibition of IRF3 phosphorylation by ORF142

To further investigate the effects of ORF142 on IFN-β production, we analyzed IRF3 phosphorylation. Vec-GFP (empty GFP) was transfected with GFP-ORF142 into Vero cells. SEV was added 12 h later to stimulate innate immunity initiation, and total proteins were extracted and analyzed by western blotting 24 h after transfection. The results showed that ORF142 inhibited the phosphorylation of IRF3 in a dose-dependent manner (Fig. 3A). Additionally, 293T, Vero, and MDBK cells were infected using LSDV WT (wild-type strain) and LSDV △142 (142 gene deletion strain) (MOI of 1), and the effect of endogenous IRF3 phosphorylation was analyzed by western blotting. The results showed that IRF3 phosphorylation was significantly inhibited in cells infected with LSDV WT compared to those infected with LSDV Δ142 (Fig. 3C–E). These findings suggested that ORF142 interferes with IRF3 activation.

ORF142 inhibits the binding of TBK1 and IRF3

At the stage of viral infection, CGAS recognizes viral DNA and activates the CGAS-STING-TBK1-IRF3 axis, thus inducing the expression of IFN-I and ISG [21, 22]. The above experiments showed that ORF142 interacts with IRF3 and inhibits its nuclear translocation. To further explore the effect of ORF142 on the CGAS-STING-TBK1-IRF3 axis, we co-transfected vec-GFP, GFP-ORF142 with Flag-TBK1, and mCherry-IRF3 into 293T cells. After 24 h, magnetic beads coupled with an anti-Flag antibody were analyzed in an immunoprecipitation assay, which showed that ORF142 inhibited the binding of TBK1 to IRF3 in a dose-dependent manner (Fig. 4A). To further confirm the role between ORF142 and IRF3, we transfected GFP-ORF142 with mCherry-IRF3 into 293T cells and set up SEV (Sendai virus) stimulation groups. Confocal microscopy image analysis showed that IRF3 was distributed in the cytoplasm

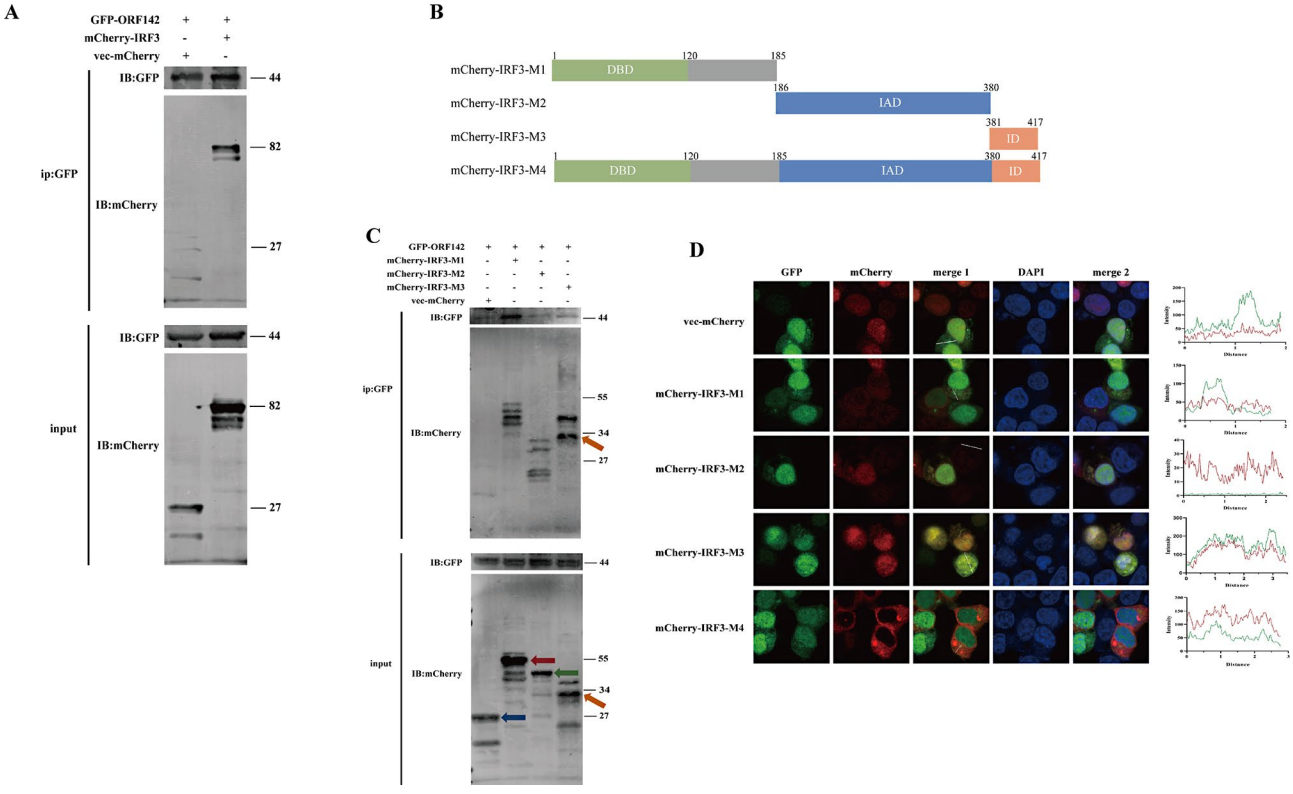

Fig. 2 ORF142 inhibits IRF3 nuclear translocation and interacts with IRF3. (**A**) GFP-ORF142 and empty plasmid vec-GFP were co-transfected with mCherry-IRF3 into 293T cells. (**B**) Schematic diagram of the full-length of IRF3 and its truncated mutants. The GFP-ORF142 and IRF3 full-length and truncated mutants were transfected into 293T cells, respectively. (**C**) Immunoprecipitation assay using magnetic beads coupled an anti-GFP antibody was performed after 24 h later and analyzed by western blotting. (**D**) Co-localization is observed by confocal microscopy after 24 h.

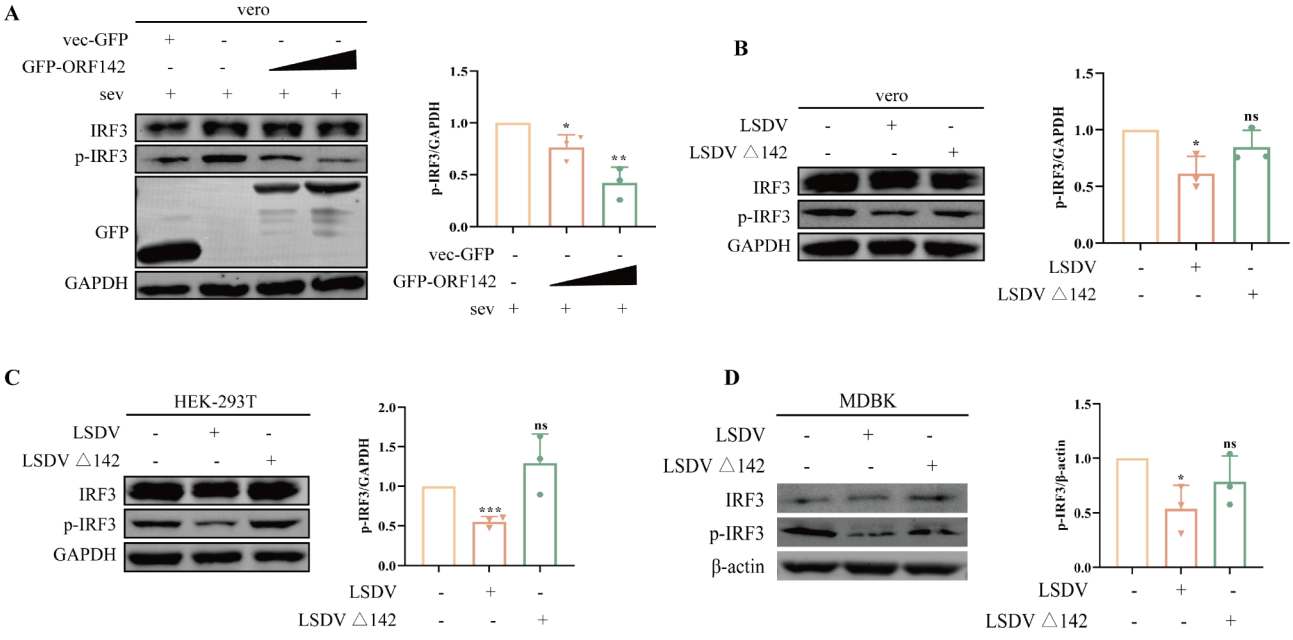

Fig. 3 ORF142 interferes with IRF3 activation. (**A**) Different doses of GFP-ORF142 plasmid (0, 0.5, and 1.5 μg) and empty plasmid vec-GFP were treated with Sendai virus (SEV) for 12 h and quantified by western blotting for p-IRF3 and IRF3 protein content. (**B**–**D**) HEK-293T, Vero, and MDBK cells were infected using a wild-type strain (LSDV WT) and a 142 gene deletion strain (LSDV △142), and the endogenous p-IRF3 and IRF3 protein levels were detected by western blotting after 24 h. GraphPad was used to determine the statistical significance and create the graphs. *$P < 0.05$, **$P < 0.01$, ***and ****$P < 0.001$.

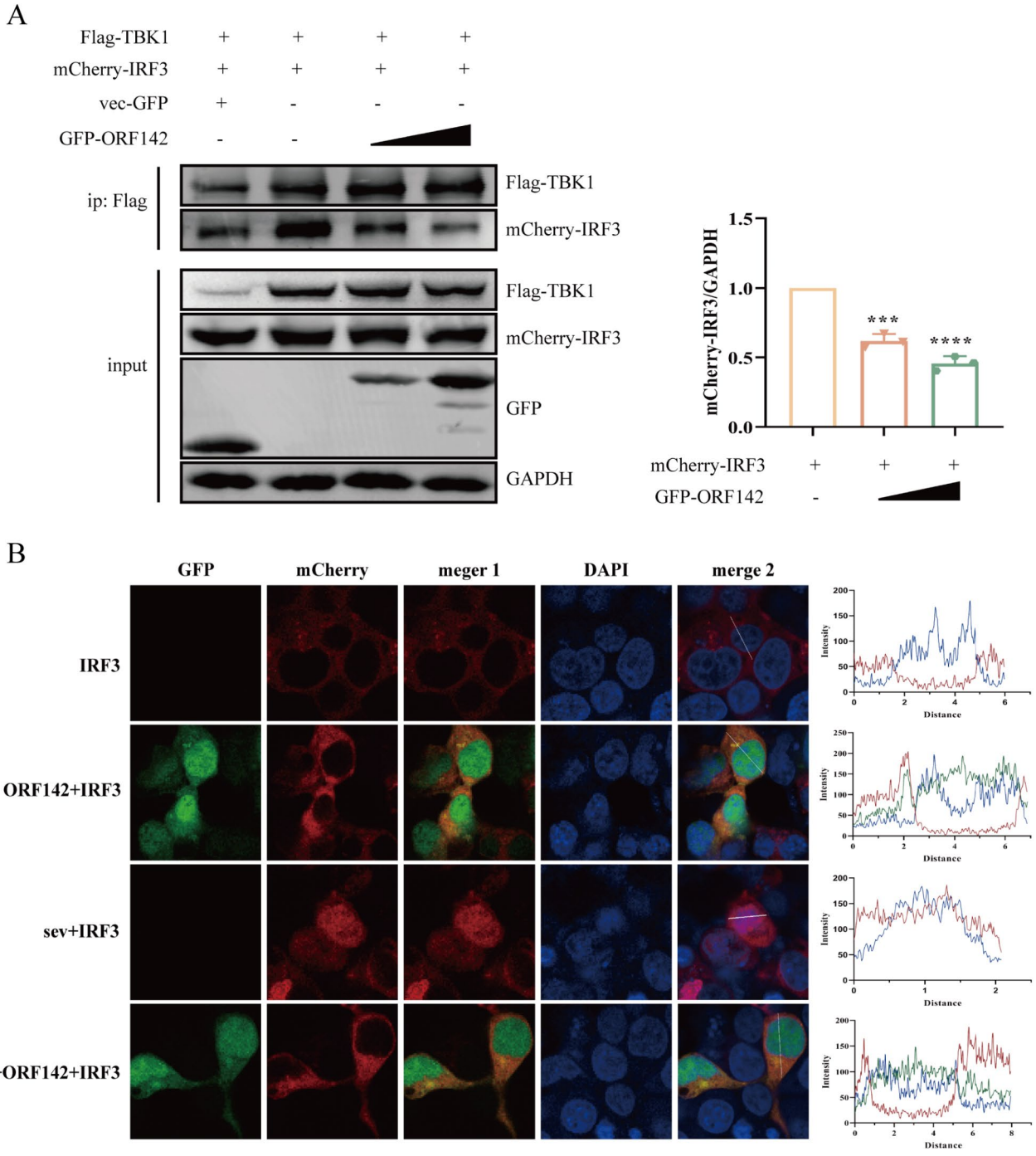

Fig. 4 ORF142 dose-dependent inhibition of TBK1 and IRF3 binding. (**A**) Co-transfection of vec-GFP and different doses of GFP-ORF142 (0, 1, and 4 μg) with Flag-TBK1 and mCherry-IRF3, respectively, into 293T cells, with a plotted mCherry-IRF3 protein content histogram. (**B**) mCherry-IRF3 is co-transfected with GFP-ORF142 while transfecting 293T cells and divided into a SEV-stimulated group (stimulated with SEV after 12 h of transfection) and an unstimulated group (left untreated after 12 h of transfection), and the localization was observed by confocal microscopy after 24 h. GraphPad was used to determine the statistical significance and create the graphs. *$P < 0.05$, **$P < 0.01$, ***and ****$P < 0.001$

of SEV-uninfected cells with or without ORF142 overexpression (Fig. 4B, rows 1 and 2). In cells infected with SEV and not overexpressing ORF142, IRF3 was efficiently translocated to the nucleus (Fig. 4B, row 3), whereas the SEV-induced nuclear translocation of IRF3 was severely impaired in cells expressing ORF142 (Fig. 4B, row 4). Therefore, LSDV ORF142 responds to viral infection by inhibiting IRF3 nuclear translocation during the viral infection phase.

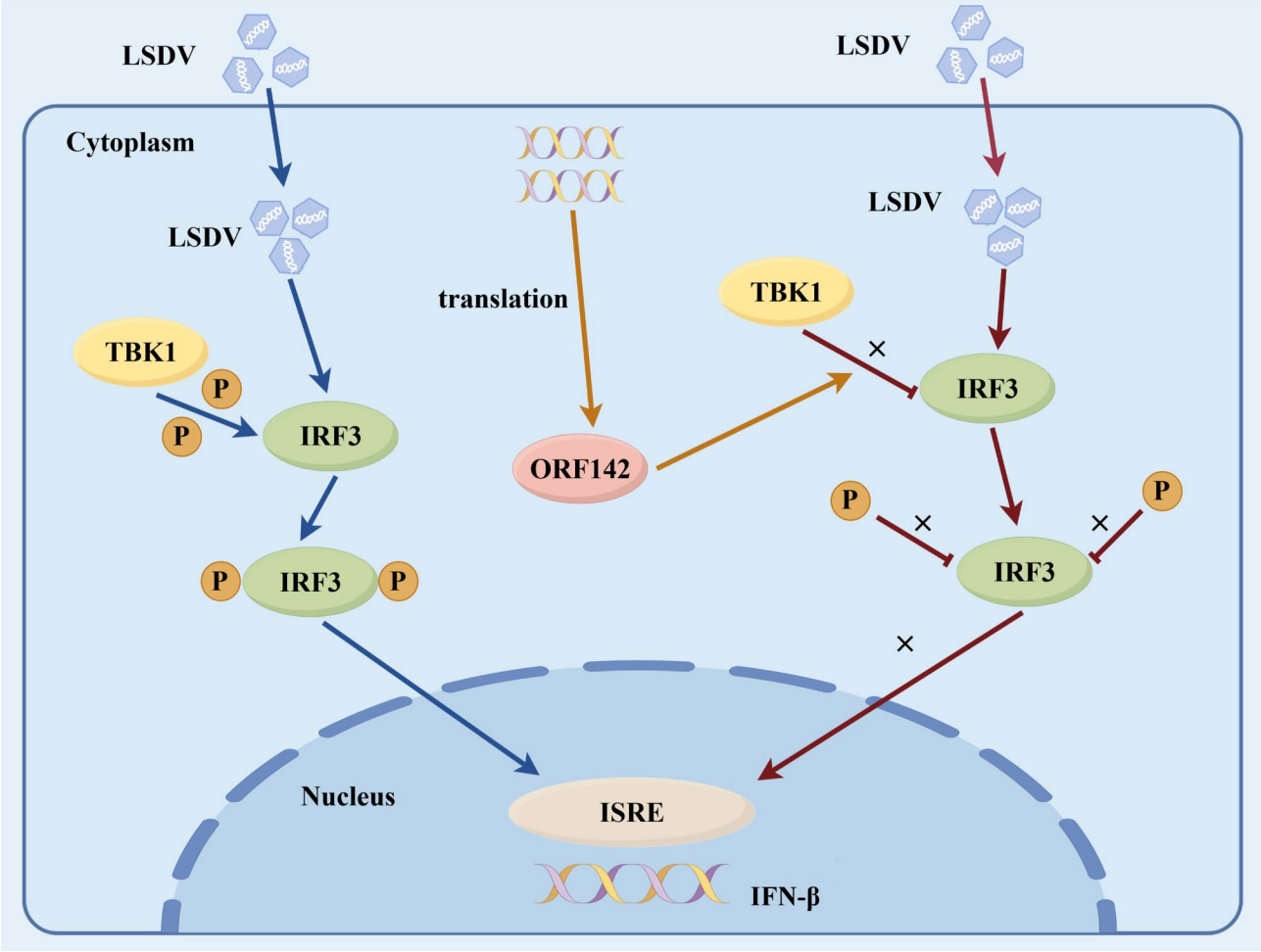

Fig. 5 Schematic diagram of the working model of the LSDV ORF142 protein negatively regulating IFN-I production. The LSDV ORF142 protein inhibits the phosphorylation of IRF3 by interacting with IRF3 and disrupting the interaction between TBK1 and IRF3, thereby inhibiting the production of IFN-I. Both wild-type LSDV and ORF142 proteins allow the virus to evade innate immunity by inhibiting the binding of TBK1 and IRF3. The diagram was created using Figdraw (https://www.figdraw.com/)

Figure 5 illustrates the mechanism by which LSDV ORF142 disrupts the TBK1-IRF3 pathway, thus inhibiting IFN-β production. In a normal antiviral response (indicated by blue arrows), LSDV infection activates the TBK1-IRF3 signaling cascade. TBK1 phosphorylates IRF3, leading to the activation and translocation of IRF3 into the nucleus, where it binds to ISRE to induce IFN-β production. However, this pathway was inhibited in the presence of ORF142 (indicated by brown arrows). The ORF142 protein, translated from LSDV RNA, binds to IRF3, preventing its interaction with TBK1 and subsequent phosphorylation. This disruption hinders the nuclear translocation of IRF3, blocking IFN-β production and allowing LSDV to evade the host's innate immune response.

Discussion

Activation of the TBK1-IRF3 complex is essential to produce IFN-β, which plays a crucial role in the host's innate immune response against viral infection. Despite its importance, the regulatory mechanisms governing the TBK1-IRF3 pathway, particularly how viruses circumvent this pathway to evade immunity, remain unclear. This study showed that the LSDV ORF142 protein interacts directly with IRF3, disrupting its association with TBK1, and preventing the nuclear translocation of IRF3. This finding identified ORF142 as a critical player in the immune evasion of LSDV, highlighting how poxviruses modulate host antiviral signaling pathways.

Innate immunity is the first line of defense against pathogens and includes various receptor-mediated pathways such as RIG-I-like receptors (RLRs), NOD-like receptors (NLRs), toll-like receptors, and the cGAS-STING pathway. Collectively, these systems restrict viral

replication, providing the host with time to mount an adaptive immune response, which is essential for viral clearance [23]. Within these pathways, IRF3 plays a central role in initiating the transcription of IFN-β and other antiviral genes upon activation [24]. However, numerous studies have revealed that many viruses have evolved specific proteins that inhibit IRF3 activation and evade the host antiviral defense. Examples include enterovirus A71, foot-and-mouth disease virus, African swine fever virus (ASFV), and herpes simplex virus type I, which each deploy unique strategies to suppress IRF3 signaling, highlighting the evolutionary pressure on viruses to target this critical antiviral factor [18, 25–27]. In our study, we found that LSDV ORF142 specifically targeted IRF3 to facilitate immune evasion. By binding to the 381–417 amino acid region of IRF3, ORF142 prevents IRF3 from undergoing phosphorylation and subsequent nuclear translocation, thus blocking the production of IFN-β and other antiviral cytokines. This interaction represents a previously uncharacterized mechanism in the poxvirus family, highlighting the unique immunomodulatory strategies of LSDV and its ability to disrupt host immune responses through targeted interference with the TBK1-IRF3 axis.

Therefore, our findings contribute to a broader understanding of the viral antagonism of IRF3. Several viruses have used various strategies to subvert IRF3 and disrupt their innate immunity. For example, the ASFV nonstructural protein D129L competitively inhibits the interaction of IRF3 with the coactivator CBP/p300 by binding directly to CBP/p300, thus preventing IFN-β production [28]. Similarly, the Zika virus NS4B interacts with TBK1, blocking IRF3 phosphorylation and its translocation to the nucleus [29]. The peste des petits ruminants virus also disrupts the TBK1-IRF3 interaction, leading to the inhibition of IRF3 nuclear translocation and IFN-β synthesis [30]. Consistent with these mechanisms, we observed that IRF3 phosphorylation was inhibited after LSDV WT infection, whereas deletion of 142 restored IRF3 phosphorylation levels. Furthermore, the expression of a GFP-tagged ORF142 construct produced a dose-dependent inhibition of IRF3 activation in multiple cell types, showing the robust immune evasion capability conferred by ORF142.

The TBK1-IRF3 axis serves as a central signaling hub in host defense against viral pathogens, primarily through the induction of IFN-I [31]. Activation of this pathway typically begins with the sensing of viral components by PRRs, such as cGAS, which detects cytoplasmic viral DNA [32, 33]. This recognition triggers the cGAS-STING pathway, leading to TBK1 activation, IRF3 phosphorylation, and ultimately IFN-β production [21]. Our study revealed that LSDV circumvents this defense mechanism by competitively binding to IRF3 and preventing TBK1 from accessing its downstream substrates. This interaction specifically suppresses the TBK1-IRF3 signaling cascade, allowing LSDV to evade early immune detection and establish infection in the host. The identification of ORF142 as a critical factor in immune suppression highlights a novel mechanism by which poxviruses subvert host defenses and underscores the importance of the TBK1-IRF3 axis in antiviral immunity.

Furthermore, recent studies have highlighted the importance of ubiquitin-mediated regulation of the TBK1-IRF3 pathway. For example, the E3 ubiquitin ligase FBXO11 has been shown to enhances IFN-I signaling by promoting TBK1 and IRF3 phosphorylation [34]. Additionally, mutant p53 binds to the TBK1-IRF3 complex, preventing the formation of the trimeric complex required for IRF3 activation, nuclear translocation, and transcriptional activity [35]. By disrupting the TBK1-IRF3 interaction, LSDV ORF142 mimics these inhibitory interactions and effectively dampens the early stages of the host's antiviral response. The shared targeting of the TBK1-IRF3 pathway by viral and cellular modulators underlines the importance of this pathway and suggests that it is a promising therapeutic target for modulating immune responses.

The implications of our findings extend beyond the field of poxvirus research, as they contribute to a broader understanding of viral immune evasion strategies that target the TBK1-IRF3 axis. Given the critical role of the TBK1-IRF3 pathway in host defense against DNA viruses, the identification of ORF142 as a potent immune antagonist suggests that similar mechanisms are conserved in related viral families. Understanding these strategies not only provides insight into the evolution of immune evasion in viruses, but also opens new avenues for therapeutic interventions. For example, small molecules or peptides that block ORF142 binding to IRF3 can be explored as potential antiviral agents to restore immune function in LSDV infections. Furthermore, enhancing the TBK1-IRF3 pathway activity through pharmacological modulation might be a viable strategy to counteract immune suppression by other poxviruses. Given that this pathway is critical for host defense against a wide range of viral pathogens, our study highlights potential therapeutic targets for improving antiviral immunity. By restoring TBK1-IRF3 signaling, it may be possible to counteract immune suppression and improve host resilience to infection, not only with LSDV, but also with other viruses, using similar mechanisms. In summary, our study uncovers a novel immune evasion mechanism employed by LSDV through ORF142-mediated disruption of the TBK1-IRF3 axis, a pathway central to antiviral defense. These findings not only advance our understanding of poxvirus-host interactions but also

highlight the potential for therapeutic strategies targeting this pathway.

Further research is needed to better dissect the molecular details of the ORF142-IRF3 interaction and explore potential inhibitors that could disrupt this interaction. This study could pave the way for new antiviral approaches aimed at preserving TBK1-IRF3 activity and bolstering the innate immune response. Therefore, this study provides a foundation for mechanistic insights and therapeutic exploration, advancing our understanding of viral pathogenesis and immune regulation. By developing agents that restore TBK1-IRF3 signaling, we may enhance host immunity against LSDV and related viruses, offering a promising avenue for combating viral infections in both veterinary and human medicine. This work underscores the importance of exploring conserved immune evasion mechanisms as targets for next-generation antiviral therapies.

Conclusion

Our study identified LSDV ORF142 as a critical viral factor that disrupts the TBK1-IRF3 pathway to evade the host's innate immune response. This study showed that ORF142 binds directly to IRF3, blocking its interaction with TBK1 and its subsequent phosphorylation and nuclear translocation, thereby effectively inhibiting IFN-β production. This immune evasion strategy highlights the sophistication of LSDV interactions with host antiviral defenses and reveals a novel mechanism by which poxviruses circumvent the key components of the innate immune system.

Methods

Cells, viruses, and antibodies

HEK-293T and Vero cell lines were obtained from the Department of Surgery, College of Veterinary Medicine, South China Agriculture University, and cultured in Dulbecco's modified Eagle's medium (DMEM) (VivaCell Biosciences, China) supplemented with 10% fetal bovine serum (FBS) (VivaCell Biosciences, China) and 100 U/mL penicillin and streptomycin. All cells were grown at 37 °C under a 5% CO_2 atmosphere.

LSDV/MZGD/2020 (OP985536.1) was isolated from domestic cattle in Guangdong, China [19] and stored in our laboratory. The wild-type LSDV (LSDV WT) stock and LSDV with 142 gene deletions (LSDV-Δ142) stock were propagated in MDBK cells in DMEM containing 2% FBS, and aliquots were stored at -80 °C.

Protease inhibitor mixture, protein phosphatase inhibitor mixture cocktail, and radio-immunoprecipitation assay (RIPA) lysis buffer were purchased from Solarbio (Beijing Solarbio Science & Technology Co., Ltd.). Mouse anti-GFP and rabbit anti-mCherry antibodies were purchased from GeneTex (Irvine, California, USA). Rabbit anti-FLAG, anti-IRF3, and anti-pIRF3 antibodies were purchased from Cell Signaling Technology (Danvers, MA, USA). Mouse anti-GAPDH and anti-β-actin antibodies were purchased from Proteintech (Wuhan, China).

Plasmid construction

All of the enzymes used for the cloning were purchased from Vazyme (Nanjing, China). Flag-IRF3, GFP-ORF142, mCherry-IRF3, and Flag-TBK1 expression plasmids were constructed using standard molecular biology techniques. The truncation mutants mCherry-IRF3-1-186aa, mCherry-IRF3-187-380aa, and mCherry-IRF3-381-417aa were synthesized by Miao LingBio, China. The other plasmids used were HA-IRF3/5D, IFNβ-Luc, interferon-stimulated response element (ISRE)-Luc, and pRL-TK.

Coimmunoprecipitation and western blotting

Cells were transfected with plasmids using Lipo™8000 Transfection Reagents (Beyotime, Shanghai, China) and Lipofectamine™3000 (Invitrogen, USA). Upon reaching 60–70% confluency, the cells were lysed using western and Co-Immunoprecipitation (Co-IP) cell lysates (Beyotime, Shanghai, China) and bound using BeyoMag™ Anti-Flag Magnetic Beads and BeyoMag™ Anti-GFP Magnetic Beads at room temperature for 2 h. For western blotting analysis, target proteins were analyzed by 10% sodium dodecyl sulfate-polyacrylamide gel electrophoresis (SDS-PAGE) and then transferred to Immobilon-Pmembrane (EMD Millipore, Billerica, MA, USA) and blocked with QuickBlock™ Western Sequestration Solution for 30 min at 37 °C. The protein bands were sequentially incubated with the corresponding primary and secondary antibodies and subsequently detected.

RNA isolation and RT-qPCR

Total RNA was extracted using the RNAfast200 Total RNA Extraction Kit (Shanghai Feijie Biotechnology Co., Ltd.). China) according to the manufacturer's instructions. Reverse transcription and qPCR reagents were sourced from Vazyme Biotech Co., Ltd. (Nanjing, China). The primers used for qPCR were as follows: IFN-β, forward, 5′-TCTTTCCATGAGCTACAACTTGCT-3′ and reverse, 5′-GCAGTATTCAAGCCTCCCATTC-3′; ISG15, forward, 5′-GGACCTGACGGTGAAGATG-3′ and reverse, 5′-AGAGGTTCGTCGCATTTGT-3′; ISG54, forward, 5′-GCCAATGATAATCTCTTCCG-3′ and reverse, 5′-TGAAAGTTGCCATACCGC-3′; ISG60, forward, 5′-GAAGGAGAGCAGTTTGTTGA-3′ and reverse, 5′-ATCTGGTGATAGAGGTAGCC-3.′.

Dual-luciferase reporter (DLR) assays

The reporter plasmids were transfected into HEK-293T cells as IFNβ-Luc, ISRE-Luc, and the internal control plasmid pRL-TK with Lipofectamine 8000 (Beyotime, China). Luciferase assays were performed 24 h post-transfection using a dual-specific luciferase assay kit (Promega, Madison, WI, USA).

Confocal microscopy techniques

After transfection and culturing to a certain density, the cells were washed three times with phosphate-buffered saline (PBS) and fixed with 4% paraformaldehyde for 10 min at room temperature. The cells were washed again and subsequently cells were stained with 4,'6-diamidino-2-phenylindole (DAPI) staining solution (Solarbio) for 10 min to visualize the nuclei. The stained cells were observed under a laser scanning microscope (Leica, Frankfurt, Germany) for detailed observation of the nuclear morphology and co-localization of target proteins by DAPI staining.

Statistical analysis

For each experiment, three independent replicates were performed to ensure the reliability and reproducibility of the results. Data from these experiments are presented as mean ± standard deviation, providing a measure of variability and central tendency. Statistical analyses to evaluate differences between groups were conducted using the t-test function in the GraphPad Prism software (version 8.0.2). Statistical significance was set at a p-value of less than 0.05, indicating a significant difference between the compared datasets.

Abbreviations

LSDV	Lumpy skin disease virus
IRF3	Interferon regulatory factor 3
LSD	Lumpy skin disease
ORFs	Open reading frames
PRRs	Pattern recognition receptors
ISGs	Interferon-stimulated genes
IFNs	Type I interferons
RIG-I	Retinoic Acid-inducible Gene-I
ITIM	Immunoreceptor tyrosine motif
ASFV	African Swine Fever Virus
DMEM	Dulbecco's modified Eagle's medium
FBS	Fetal bovine serum
RIPA	Radio-immunoprecipitation assay
ISRE	Interferon-stimulated response element
Co-IP	Co-Immunoprecipitation
SDS-PAGE	Sodium dodecyl sulfate-polyacrylamide gel electrophoresis
DLR	Dual-luciferase reporter
PBS	Phosphate-buffered saline
DAPI	4,'6-diamidino-2-phenylindole
SEV	Sendai virus
WT	Wild-type strain
RLRs	RIG-I-like receptors

Supplementary Information

The online version contains supplementary material available at https://doi.org/10.1186/s12917-025-04714-y.

Supplementary Material 1

Supplementary Material 2

Supplementary Material 3

Supplementary Material 4

fig 1

fig 2

fig 3

fig 5

Acknowledgements

We would like to thank our colleagues and co-authors at the School of Veterinary Medicine, South China Agricultural University, for their collaboration in the LSDV study.

Author contributions

Zihan Chen contributed to the editing process, refining the language, improving clarity, and ensuring adherence to academic writing standards; Jingyu Wang was instrumental in the initial conception of the research idea and collaborated with team members to devise the research framework and hypotheses; Baochun Lu played a pivotal role in setting research objectives, selecting methodologies, and determining data collection strategies; Heyu Li was responsible for conducting fieldwork/experiments, ensuring the validity and reliability of the collected data; Chuanli Liu conducted in-depth data analysis, employing statistical techniques to derive meaningful insights from the collected data; Huijuan Zeng contributed to the editing process, refining the language, improving clarity, and ensuring adherence to academic writing standards; Jinping Chen served as the project manager, coordinating tasks among team members, ensuring timelines were met, and facilitating communication; Shizhe Liu conducted an extensive literature review, synthesizing existing knowledge to establish a theoretical foundation for the study; Qifeng Jiang took primary responsibility for drafting the manuscript, ensuring that it flowed logically and presented the research findings clearly; Kun Jia served as the project manager, coordinating tasks among team members, ensuring timelines were met, and facilitating communication and also handled administrative tasks, such as obtaining necessary permissions and managing project budgets; All the authors reviewed, wrote, and revised the manuscript.

Funding

This study was supported by the Guangzhou Municipal Science and Technology Project (grant numbers: 2023E04J0106 and 202206010131). Funding bodies did not play a role in the design of the study, collection, analysis, and interpretation of the data, or in the writing of the manuscript.

Data availability

No datasets were generated or analysed during the current study.

Declarations

Ethics approval and consent to participate

Not applicable.

Consent for publication

Not applicable.

Competing interests

The authors declare no competing interests.

Received: 10 January 2025 / Accepted: 26 March 2025
Published online: 09 April 2025

References

1. Akther M, Akter SH, Sarker S, Aleri JW, Annandale H, Abraham S, Uddin JM. Global burden of lumpy skin disease, outbreaks, and future challenges. VIRUSES-BASEL 2023, 15(9).
2. Sumana K, Revanaiah Y, Shivachandra SB, Mothay D, Apsana R, Saminathan M, Basavaraj S, Reddy G. Molecular phylogeny of capripoxviruses based on major immunodominant protein (P32) reveals circulation of host specific sheeppox and goatpox viruses in small ruminants of India. INFECT GENET EVOL. 2020;85:104472.
3. Kononova S, Kononov A, Shumilova I, Byadovskaya O, Nesterov A, Prutnikov P, Babiuk S, Sprygin A. A lumpy skin disease virus which underwent a recombination event demonstrates more aggressive growth in primary cells and cattle than the classical field isolate. TRANSBOUND EMERG DIS. 2021;68(3):1377–83.
4. Tulman ER, Afonso CL, Lu Z, Zsak L, Kutish GF, Rock DL. Genome of lumpy skin disease virus. J VIROL. 2001;75(15):7122–30.
5. Wang J, Ji J, Zhong Y, Meng W, Wan S, Ding X, Chen Z, Wu W, Jia K, Li S. Construction of Recombinant fluorescent LSDV for high-throughput screening of antiviral drugs. VET RES. 2024;55(1):33.
6. Wang J, Lu W, Zhang J, Du Y, Fang M, Zhang A, Sungcad G, Chon S, Xing J. Loss of TRIM29 mitigates viral myocarditis by attenuating PERK-driven ER stress response in male mice. NAT COMMUN. 2024;15(1):3481.
7. Al HM, Brady G. Regulation of IRF3 activation in human antiviral signaling pathways. BIOCHEM PHARMACOL. 2022;200:115026.
8. Hare DN, Baid K, Dvorkin-Gheva A, Mossman KL. Virus-Intrinsic differences and heterogeneous IRF3 activation influence IFN-Independent antiviral protection. ISCIENCE. 2020;23(12):101864.
9. Santhamani R, Yogisharadhya R, Venkatesan G, Shivachandra SB, Pandey AB, Ramakrishnan MA. Molecular characterization of Indian sheeppox and goatpox viruses based on RPO30 and GPCR genes. Virus Genes. 2014;49(2):286–91.
10. Chibssa TR, Kangethe RT, Berguido FJ, Settypalli T, Liu Y, Grabherr R, Loitsch A, Sassu EL, Pichler R, Cattoli G, et al. Innate immune responses to wildtype and attenuated sheeppox virus mediated through RIG-1 sensing in PBMC In-Vitro. FRONT IMMUNOL. 2021;12:666543.
11. Liang Z, Wang S, Yao K, Ren S, Cheng P, Qu M, Ma X, Gao X, Yin X, Wang X, et al. Lumpy skin disease virus ORF127 protein suppresses type I interferon responses by inhibiting K63-linked ubiquitination of tank binding kinase 1. FASEB J. 2024;38(3):e23467.
12. Ishikawa H, Barber GN. STING is an Endoplasmic reticulum adaptor that facilitates innate immune signalling. Nature. 2008;455(7213):674–8.
13. Fang M, Zhang A, Du Y, Lu W, Wang J, Minze LJ, Cox TC, Li XC, Xing J, Zhang Z. TRIM18 is a critical regulator of viral myocarditis and organ inflammation. J BIOMED SCI. 2022;29(1):55.
14. Fitzgerald KA, McWhirter SM, Faia KL, Rowe DC, Latz E, Golenbock DT, Coyle AJ, Liao SM, Maniatis T. IKKepsilon and TBK1 are essential components of the IRF3 signaling pathway. NAT IMMUNOL. 2003;4(5):491–6.
15. Chen H, Sun H, You F, Sun W, Zhou X, Chen L, Yang J, Wang Y, Tang H, Guan Y, et al. Activation of STAT6 by STING is critical for antiviral innate immunity. Cell. 2011;147(2):436–46.
16. Wang Y, Qian G, Zhu L, Zhao Z, Liu Y, Han W, Zhang X, Zhang Y, Xiong T, Zeng H, et al. HIV-1 Vif suppresses antiviral immunity by targeting STING. CELL MOL IMMUNOL. 2022;19(1):108–21.
17. Liu H, Ye G, Liu X, Xue M, Zhou Q, Zhang L, Zhang K, Huang L, Weng C. Vimentin inhibits type I interferon production by disrupting the TBK1-IKKε-IRF3 axis. CELL REP. 2022;41(2):111469.
18. Liu H, Zhu Z, Feng T, Ma Z, Xue Q, Wu P, Li P, Li S, Yang F, Cao W, et al. African swine fever virus E120R protein inhibits interferon beta production by interacting with IRF3 to block its activation. J VIROL. 2021;95(18):e82421.
19. Wang J, Xu Z, Wang Z, Li Q, Liang X, Ye S, Cheng K, Xu L, Mao J, Wang Z, et al. Isolation, identification and phylogenetic analysis of lumpy skin disease virus strain of outbreak in Guangdong, China. TRANSBOUND EMERG DIS. 2022;69(5):e2291–301.
20. Zevini A, Olagnier D, Hiscott J. Crosstalk between cytoplasmic RIG-I and STING sensing pathways. TRENDS IMMUNOL. 2017;38(3):194–205.
21. Chen Q, Sun L, Chen ZJ. Regulation and function of the cGAS-STING pathway of cytosolic DNA sensing. NAT IMMUNOL. 2016;17(10):1142–9.
22. Balka KR, De Nardo D. Molecular and Spatial mechanisms governing STING signalling. FEBS J. 2021;288(19):5504–29.
23. McNab F, Mayer-Barber K, Sher A, Wack A, O'Garra A. Type I interferons in infectious disease. NAT REV IMMUNOL. 2015;15(2):87–103.
24. Navarro L, David M. p38-dependent activation of interferon regulatory factor 3 by lipopolysaccharide. J BIOL CHEM. 1999;274(50):35535–8.
25. Ji W, Sun T, Li D, Chen S, Yang H, Jin Y, Duan G. TBK1 and IRF3 are potential therapeutic targets in enterovirus A71-associated diseases. PLOS Negl TROP D. 2023;17(1):e11001.
26. Liu H, Xue Q, Yang F, Cao W, Liu P, Liu X, Zhu Z, Zheng H. Foot-and-mouth disease virus VP1 degrades YTHDF2 through autophagy to regulate IRF3 activity for viral replication. AUTOPHAGY. 2024;20(7):1597–615.
27. You H, Zheng S, Huang Z, Lin Y, Shen Q, Zheng C. Herpes Simplex Virus 1 Tegument Protein UL46 Inhibits TANK-Binding Kinase 1-Mediated Signaling. MBIO 2019, 10(3).
28. Zhang K, Ge H, Zhou P, Li L, Dai J, Cao H, Luo Y, Sun Y, Wang Y, Li J, et al. The D129L protein of African swine fever virus interferes with the binding of transcriptional coactivator p300 and IRF3 to prevent beta interferon induction. J VIROL. 2023;97(10):e82423.
29. Sarratea MB, Alberti AS, Redolfi DM, Truant SN, Iannantuono LL, Bivona AE, Mariuzza RA, Fernandez MM, Malchiodi EL. Zika virus NS4B protein targets TANK-binding kinase 1 and inhibits type I interferon production. BBA-GEN Subj. 2023;1867(12):130483.
30. Zhu Z, Li P, Yang F, Cao W, Zhang X, Dang W, Ma X, Tian H, Zhang K, Zhang M et al. Peste des Petits Ruminants Virus Nucleocapsid Protein Inhibits Beta Interferon Production by Interacting with IRF3 To Block Its Activation. J VIROL: 2019, 93(16).
31. Wu H, Yan X, Zhao L, Li X, Li X, Zhang Y, Gu C, Yang F, Yan J, Lou Y, et al. p120-catenin promotes innate antiviral immunity through stabilizing TBK1-IRF3 complex. MOL IMMUNOL. 2023;157:8–17.
32. Xing J, Weng L, Yuan B, Wang Z, Jia L, Jin R, Lu H, Li XC, Liu Y, Zhang Z. Identification of a role for TRIM29 in the control of innate immunity in the respiratory tract. NAT IMMUNOL. 2016;17(12):1373–80.
33. Xing J, Zhang A, Zhang H, Wang J, Li XC, Zeng M, Zhang Z. TRIM29 promotes DNA virus infections by inhibiting innate immune response. NAT COMMUN. 2017;8(1):945.
34. Gao L, Gao Y, Han K, Wang Z, Meng F, Liu J, Zhao X, Shao Y, Shen J, Sun W, et al. FBXO11 amplifies type I interferon signaling to exert antiviral effects by facilitating the assemble of TRAF3-TBK1-IRF3 complex. J MED VIROL. 2023;95(3):e28655.
35. Zhang H, Han C, Li T, Li N, Cao X. The methyltransferase PRMT6 attenuates antiviral innate immunity by blocking TBK1-IRF3 signaling. CELL MOL IMMUNOL. 2019;16(10):800–9.

Publisher's note